



UvA-DARE (Digital Academic Repository)

Characterization of monoclonal antibody charge variants under near-native separation conditions using nanoflow sheath liquid capillary electrophoresis-mass spectrometry

Zon, A.A.M. van der; Höchsmann, A.; Bos, T.S.; Neusüß, C.; Somsen, G.W.; Jooß, K.; Haselberg, R.; Gargano, A.F.G.

DOI

[10.1016/j.aca.2024.343287](https://doi.org/10.1016/j.aca.2024.343287)

Publication date

2024

Document Version

Final published version

Published in

Analytica Chimica Acta

License

CC BY

[Link to publication](#)

Citation for published version (APA):

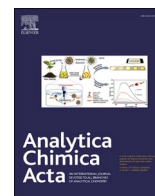
Zon, A. A. M. V. D., Höchsmann, A., Bos, T. S., Neusüß, C., Somsen, G. W., Jooß, K., Haselberg, R., & Gargano, A. F. G. (2024). Characterization of monoclonal antibody charge variants under near-native separation conditions using nanoflow sheath liquid capillary electrophoresis-mass spectrometry. *Analytica Chimica Acta*, 1331, Article 343287. <https://doi.org/10.1016/j.aca.2024.343287>

General rights

It is not permitted to download or to forward/distribute the text or part of it without the consent of the author(s) and/or copyright holder(s), other than for strictly personal, individual use, unless the work is under an open content license (like Creative Commons).

Disclaimer/Complaints regulations

If you believe that digital publication of certain material infringes any of your rights or (privacy) interests, please let the Library know, stating your reasons. In case of a legitimate complaint, the Library will make the material inaccessible and/or remove it from the website. Please Ask the Library: <https://uba.uva.nl/en/contact>, or a letter to: Library of the University of Amsterdam, Secretariat, P.O. Box 19185, 1000 GD Amsterdam, The Netherlands. UvA-DARE is a service provided by the library of the University of Amsterdam (<https://dare.uva.nl>). You will be contacted as soon as possible.



Characterization of monoclonal antibody charge variants under near-native separation conditions using nanoflow sheath liquid capillary electrophoresis-mass spectrometry

Annika A.M. van der Zon^{a,b,*}, Alisa Höchsmann^{c,d}, Tijmen S. Bos^{a,b}, Christian Neusüß^c, Govert W. Somsen^{b,e}, Kevin Jooß^{b,e,*}, Rob Haselberg^{b,e,*}, Andrea F.G. Gargano^{a,b,*}

^a University of Amsterdam, van 't Hoff Institute for Molecular Sciences, Analytical Chemistry Group, Science Park 904, 1098 XH, Amsterdam, the Netherlands

^b Centre of Analytical Sciences Amsterdam, Science Park 904, 1098 XH, Amsterdam, the Netherlands

^c Aalen University, Department of Chemistry, Beethovenstraße 1, 73430, Aalen, Germany

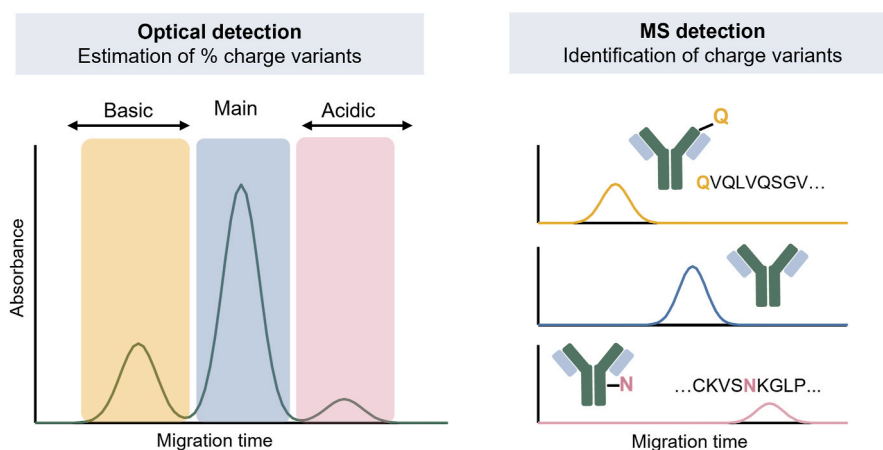
^d Eberhard Karls University of Tübingen, Faculty of Science, 72074, Tübingen, Germany

^e Vrije Universiteit Amsterdam, Department of Chemistry and Pharmaceutical Sciences, Amsterdam Institute of Molecular and Life Sciences, Division of BioAnalytical Chemistry, De Boelelaan 1085, 1081 HV, Amsterdam, the Netherlands

HIGHLIGHTS

- A CZE-UV/MS method to analyze the charge heterogeneity of intact mAbs was developed.
- A static neutral HPMC coating was used in combination with volatile BGEs at pH 5.0
- The nanoCEasy interface was implemented to allow for MS coupling.
- In-depth charge variants characterization of mAbs is accomplished.

GRAPHICAL ABSTRACT



ARTICLE INFO

Keywords:

Monoclonal antibodies
Charge heterogeneity
Capillary zone electrophoresis
Mass spectrometry

ABSTRACT

Background: Monoclonal antibodies (mAbs) undergo multiple post-translational modifications (PTMs) during production and storage, resulting for instance in charge and oxidized variants. PTMs need to be assessed as critical quality attributes to assure protein quality and safety. Capillary zone electrophoresis (CZE) enables efficient charge-based separation. The CZE method developed by He et al. (2011) is currently applied routinely in the pharmaceutical industry for profiling charge heterogeneity of mAbs. However, as the method relies on a non-

* Corresponding authors. Centre of Analytical Sciences Amsterdam, Science Park 904, 1098 XH, Amsterdam, the Netherlands.

E-mail addresses: a.a.m.vanderzon@uva.nl (A.A.M. van der Zon), k.jooss@vu.nl (K. Jooß), rob.haselberg@vectorytx.com (R. Haselberg), a.gargano@uva.nl (A.F.G. Gargano).

<https://doi.org/10.1016/j.aca.2024.343287>

Received 19 July 2024; Received in revised form 24 September 2024; Accepted 27 September 2024

Available online 9 October 2024

0003-2670/© 2024 The Author(s). Published by Elsevier B.V. This is an open access article under the CC BY license (<http://creativecommons.org/licenses/by/4.0/>).

volatile background electrolyte (BGE), it cannot be directly hyphenated with mass spectrometry (MS), hampering the identification of separated charge variants.

Results: This study presents a CZE-UV/MS method using a neutral static capillary coating of hydroxypropyl methylcellulose combined with a volatile BGE at pH 5.0 to allow for MS-compatible mAb charge variant separations. The effect of several parameters, including pH and concentration of the BGE, applied voltage, and injected mAb concentrations on separation performance was investigated using a panel of commercially available mAbs. The optimized method was evaluated with IgG₁ and IgG₄ mAbs of varying pI (7.4–9.2) and degrees of heterogeneity. Basic and acidic variants were separated from the parent mAb using a BGE of 50 mM acetic acid adjusted to pH 5.0 with ammonium hydroxide. The relative abundances of charge variants determined with the new method showed a good correlation with the corresponding relative levels obtained with the method of He et al. CZE-MS coupling was accomplished using the nanoCEasy, a low-flow sheath liquid interface, which enabled the identification and quantitation of basic, acidic, and incomplete pyroglutamate variants, and glycoforms of the tested mAbs.

Significance: This manuscript describes a new CZE-MS method that permits heterogeneity assessment of mAbs under MS-compatible conditions, providing charge variant separation.

1. Introduction

Monoclonal antibodies (mAbs) are a growing class of therapeutic agents used to treat several major diseases [1]. mAbs are complex and heterogeneous proteins consisting of two light and two heavy oligopeptide chains connected via disulfide bridges. In addition, mAbs typically possess two or more glycosylation sites. During manufacturing and storage, mAbs can undergo multiple enzymatic and chemical post-translational modifications (PTMs). The presence or quantity of these modifications can impact the efficacy and safety of the biopharmaceutical product [2]. In this context, critical quality attributes (CQAs) are a set of carefully defined product characteristics that represent an important measure to ensure product quality. One of these CQAs is charge heterogeneity, which encompasses both acidic proteoforms (originating from deamidation, sialylation, and glycation) and basic proteoforms (e.g., incomplete lysine clipping, N-terminal glutamine/pyroglutamate conversion, and succinimide formation) [3,4]. Variation in charge heterogeneity has been shown to alter the *in vitro* and *in vivo* properties of mAbs [5]. To characterize their proteoforms, mAbs are typically analyzed via bottom-up (peptide level), middle-up (subunit level), or intact protein approaches [6]. Charge variant analysis (CVA) is commonly conducted at the intact proteoform level. It requires limited sample preparation (typically only buffer exchange and/or dilution) avoiding the induction of additional modifications [7].

Several techniques have been described for CVA of biopharmaceuticals, such as ion-exchange chromatography [8] and capillary electrophoresis (CE) [9]. Within CE-based separation methods, capillary isoelectric focusing (cIEF) and capillary zone electrophoresis (CZE) are the most widely applied approaches for CVA [10–12]. The latter is a well-established and accepted technique for CVA of mAb in the pharmaceutical industry. Selectivity in CZE is based on differences in electrophoretic mobility, which is determined by molecular charge and hydrodynamic radius or, more precisely, a protein's charge-to-size ratio [13]. CZE is highly suitable to probe minor changes in the overall protein's charge. For efficient protein separation, the choice of an adequate capillary coating and background electrolyte (BGE) composition (type, pH, and ionic strength) is essential. By suppressing the electroosmotic flow (EOF) and adjusting the pH of the BGE to be close to the pI of the mAbs, the relative charge difference, and thus resolution, between proteoforms can be maximized [14]. However, when the pH is too close to the protein pI, electrophoretic migration will be very slow and solubility issues could occur [15–17].

In 2011, He et al. introduced a CVA method based on CZE with UV absorbance detection which employed a dynamically coated fused-silica capillary using a BGE comprising of 400 mM ϵ -amino-caproic acid (EACA), 2 mM triethylenetetramine (TETA), and 0.05 % m/v (hydroxypropyl) methylcellulose (HPMC) [18]. This method enables the separation of minor charge variants from the main isoform at pH 5.7. Its performance has been extensively validated and the approach has

gained prominence for CVA in the pharmaceutical industry [19]. Although this CZE-UV method is efficient for quantification purposes in a quality control environment, it is not compatible with mass spectrometric detection and, therefore, does not allow the identification of separated peaks beyond the assignment of their acidic or basic nature. This limitation is rooted in the use of non-volatile BGE constituents, which interfere with electrospray ionization (ESI), potentially causing ion suppression and contamination of the mass spectrometer [20].

The combination of CE and MS is a valuable approach to facilitate the characterization of closely related and/or minor proteoforms that are difficult to distinguish by MS alone. In particular, cIEF offers high-resolution separations of charge variants. However, the coupling of cIEF to MS is considered more complex, as ampholytes are often present in high concentrations and cause substantial MS ionization suppression [11,21]. Hence, a compromise must be reached between optimizing the separation efficiency of the cIEF step and maximizing the sensitivity of MS detection when directly integrating both techniques [22]. CZE separations, in some cases, may not offer the same resolving power as cIEF but are realized without using ampholytes and, therefore, use more MS-compatible conditions. Various CZE-MS methods for mAb analysis have been proposed, but the majority of these methods are performed using acidic BGEs (typically acetic or formic acid at pH 2–3) yielding limited to no separation of charge variants [23]. In so-called native CZE-MS, a higher pH (i.e., close to pH 7) is used [24]. However, these studies have primarily focused on the separation of different proteins rather than CVA so far. CZE-MS methods applying a BGE between pH 5–7 (here referred to as near-native) are less common [25–27]. One notable exception is the use of a commercial microfluidic CZE-MS system in combination with an MS-compatible BGE at a pH of 5.5, closely resembling the conditions of the EACA-based CZE-UV method of He et al. (2011) [28–31]. The microfluidic-CZE-MS system provides high-throughput CVA but lacks optical detection, which limits its quantitative abilities. A flexible capillary-based CZE method that enables mAb variant quantification at pH 5–6 via UV detection while also offering coupling with MS for identification has not been described yet.

In this study, we aimed to close this gap by developing a CZE-UV/MS system for intact mAb CVA. It makes use of a static neutral HPMC coating in order to prevent protein adsorption and suppress the EOF to enhance electrophoretic resolution [32]. To couple the CZE method with MS, we applied a recently introduced ESI nanoflow sheath liquid interface, referred to as “nanoCEasy” [33]. This interface results in higher detection sensitivity compared to traditional sheath liquid interfacing, enabling the detection of low-abundant proteoforms. In addition, the easy manipulation of the separation capillary and sheath liquid capillaries facilitates efficient capillary washing and BGE replacement during successive runs. In this study, the pH and concentration of the BGE, applied CZE voltage, and injected quantity of mAb were evaluated and optimized using CZE-UV. Subsequently, the potential of the CZE-nanoCEasy-MS system for the identification of resolved

charge variants was investigated. The performance of the optimized CZE-MS method was evaluated by the analysis of various immunoglobulin G (IgG) subclasses (IgG₁ and IgG₄) with isoelectric points (pI) between 7.4 and 9.2 and diverse degrees of heterogeneity.

2. Experimental section

2.1. Chemicals

Methanol, isopropanol (MS-grade), water (MS-grade), and formic acid (MS-grade) were purchased from Biosolve (Valkenswaard, The Netherlands). Ammonium hydroxide solution (25 %), and hydrochloric acid (37 %) were acquired from Merck KGaA (Darmstadt, Germany). Sodium hydroxide, hydrofluoric acid (HF) (50.5 %), calcium carbonate, HPMC, acrylamide, EACA, and TETA were purchased from Sigma-Aldrich (Zwijndrecht, The Netherlands). Acetic acid (glacial, p.a.) was purchased from Acros Organics (Geel, Belgium). Pembrolizumab, rituximab, and cetuximab were received from Amsterdam University Medical Center Pharmacy (Amsterdam, The Netherlands). Pembrolizumab (Keytruda®) was from MSD (Kenilworth, New Jersey, USA). Rituximab (Trukima®) was from Celltrion Healthcare (Amsterdam, The Netherlands), and cetuximab (Erbix®) was from Merck KGaA (Darmstadt, Germany). NISTmAb (reference material 8671, humanized IgG_{1k} monoclonal antibody) was purchased from the National Institute of Standards and Technology (Gaithersburg, Maryland, USA). Unless stated otherwise, the mAb samples were diluted to 1 mg·mL⁻¹ in water.

2.2. Coating of separation capillary

For coating the inner capillary wall with HPMC, a procedure from Shen and Smith was adopted [34]. A bare fused silica capillary (50 μm i. d., 365 μm o. d., 60 cm as total length) was purchased from Polymicro Technologies (Phoenix, USA). The capillary was initially washed with methanol followed by flushing with water, 0.1 M sodium hydroxide, water, 0.1 M hydrochloric acid, and water at 100 μL·h⁻¹ for 5 min each by using a syringe pump (kdScientific Legato™ 200, Massachusetts, USA). Hereafter, 0.75 % (w/v) HPMC solution was led through the capillary with a flow rate of 20 μL·h⁻¹ for 40 min. Subsequently, the capillary was installed in a gas chromatography oven (Agilent Technologies, Waldbronn, Germany). A heated nitrogen flow (3.5 bar) was applied for 45 min after an initial ramp from 25 to 150 °C at 5 °C·min⁻¹. After cooling down to room temperature, each coated capillary was evaluated prior to analysis by measuring the EOF at +30 kV applied voltage with 20 mM acrylamide as an EOF marker. The BGE was 50 mM acetic acid adjusted to pH 5.0 using ammonium hydroxide. During the EOF measurements, pressures varying from 10 to 100 mbar were applied to move EOF in the direction of the detector. The coating was used when the EOF was lower than 10⁻⁹ m²·v⁻¹·s⁻¹ at pH 5.0.

2.3. Etching of separation capillary

2.3.1. Safety precautions

HF is dangerous! Use appropriate safety procedures when working with HF. Make use of a fume hood. Ensure that a calcium gluconate gel (2.5 %) is nearby in case of exposure.

For CZE-MS, the CE capillary was etched. The polyimide layer was burnt off at 20 mm of the capillary outlet end using a lighter. Subsequently, the bare fused silica capillaries end was etched with HF (50.5 %) over a length of 10 mm as reported elsewhere [33]. The outlet opening was closed using a hot glue droplet to prevent the HF from accessing the capillary. The outlet end of the capillary was emersed in HF for approximately 1 h to reduce the outer diameter of the capillary to <150 μm. Note that polyimide should not come in contact with HF. To stop the reaction, the capillary was dipped in a saturated calcium carbonate solution to neutralize the HF and then washed with water. Before the CZE measurements, the blocked end with the glue droplet was cut

off.

2.4. Instrumentation

2.4.1. CZE-UV

An Agilent 7100 CE system equipped with a diode array detector (DAD) (Agilent Technologies, Waldbronn, Germany) was used. The final BGE consisted of 50 mM acetic acid adjusted to pH 5.0 using ammonium hydroxide (~5.9 mM). Other BGEs in this study were prepared in a similar fashion. Prior to each measurement, the capillary was conditioned by flushing with BGE for 200 s at 950 mbar. The samples were hydrodynamically injected for 5 s at 50 mbar (6.39 nL) followed by a BGE plug (5 s, 50 mbar). High voltage (normal polarity mode) was ramped up to 25 kV in 0.2 min (generating a current of 30–35 μA). The maximum current was set to 60 μA to avoid Joule heating. The capillary cassette temperature was set to 20 °C. The mAbs were detected at 214 nm with a data acquisition rate of 2.5 Hz. For storage of the capillary, the capillary was flushed with water and subsequently with air (300 s, 950 mbar) and stored at ambient temperature.

2.4.2. CZE-MS

The Agilent 7100 CE system was also used for CZE-MS measurements. The nanoCEasy interface was used to hyphenate the CE instrument to a Q Exactive Plus mass spectrometer (Thermo Fisher Scientific, Bremen, Germany). In Supplementary Information, Figs. S1 and S2 show the configuration of the nanoCEasy interface. Briefly, the nanoCEasy interface employs two modes: (i) conditioning mode in which the separation capillary is moved backward during flushing of the BGE, and (ii) separation mode in which the separation capillary is moved forward to around 1 mm from the emitter tip [33]. Glass emitters with a length of 55 mm, a length point of 3 mm, and an emitter i. d. of about ~30 μm were used (Biomedical Instruments Pipettes, Zöllnitz, Germany). The distance between the emitter tip and the MS orifice was set to 3 mm. The second capillary (100 μm i. d., 245 μm o. d., 30 cm length) was filled with sheath liquid composed of 0.5 % (v/v) formic acid in 50/50 isopropanol/water. A syringe pump was used with a flow rate of 10 μL·min⁻¹. The nanoCEasy setup was controlled using a digital microscope (Dino-Lite, Almere, The Netherlands). For MS, the electrospray voltage was 2.1 kV (positive ion mode), microscans were set to 10 ms, in-source CID was 80 eV, sweep gas flow rate was 3 Arb, capillary temperature was 275 °C, S-lens RF level was 100, and scan range was set to high mass range (HMR) of 1500 to 6000 *m/z* with a resolution of 17,000. The CE voltage was ramped up to 20 kV (normal polarity) in 0.2 min (generating a current of 30–35 μA).

2.4.3. EACA-based CZE-UV method

The EACA-based method using a BGE of 400 mM EACA, 2 mM TETA, and 0.05 % (w/v) HPMC at pH 5.7 was used as reported by He et al. with the calculated settings for an Agilent 7100 CE system of Wiesner et al. to make a fair comparison with the MS compatible method [18,19]. A bare fused-silica capillary (50 μm i. d., 365 μm o. d., 60 cm total length) was used. The separation voltage was ramped up from 0 to 30 kV in 0.20 min. The capillary cassette temperature was set to 25 °C. The samples were injected by applying 35 mbar for 5 s. The UV detector was set to 214 nm with 10 Hz as data acquisition rate.

2.5. Data processing

CE-UV data were processed and integrated using OpenLAB CDS software (Agilent Technologies, Waldbronn, Germany). For visualization purposes, baseline correction was executed utilizing the arPLS algorithm [35]. Previous studies have demonstrated the efficacy of this algorithm across diverse experimental conditions [36]. The raw MS data were visualized in Thermo Fisher Scientific Freestyle software (Thermo Fisher Scientific, Bremen, Germany). For the deconvolution of the spectra and calculation of the average mass, Unidec (University of

Arizona, Phoenix, USA) was used by applying the following parameters: a sample mass rate of 0.1 Da, a picking range of 1 Da, and a picking threshold of 0.05 [37]. CZE-MS data are available at MassIVE: DOI:10.25345/C5377662N.

3. Results and discussion

Four different mAbs were selected to evaluate whether the proposed method can assess various common modifications. The selected antibodies were rituximab, cetuximab, NISTmAb, and pembrolizumab. Together, they span a broad pI range (7.4–9.4), various subclasses (IgG₁ and IgG₄), and a large diversity of PTMs (e.g., sialylation, deamidation, incomplete C-terminal lysine clipping). Table S1 summarizes their properties in more detail.

3.1. EOF suppression by HPMC coating

Efficient intact protein analysis requires the use of coated capillaries in order to minimize protein interaction with the capillary wall as protein interaction may lead to band broadening or even complete protein adsorption [38]. In this study, an HPMC-coated capillary was employed. This coating also suppresses the EOF ($\mu_{\text{EOF}} \approx 0$), thereby potentially allowing efficient electrophoretic separation of the charge variants based on their difference in mobility [38].

The suppression of EOF by the HPMC-coated capillaries was evaluated by repeatedly ($n = 3$) analysis of acrylamide (EOF marker) using a voltage of +30 kV while applying pressures ranging from 10 to 100 mbar. The BGE was 50 mM acetic acid adjusted to pH 2.8 or 5.0 with ammonium hydroxide. The EOF velocity was calculated by plotting the reciprocal measured migration times of acrylamide against the applied pressure and extrapolating to zero pressure (Fig. S3). Both at 50 mM acetic acid pH 2.8 and pH 5.0, the EOF was very small (respectively, $7.5 \cdot 10^{-10} \text{ m}^2 \cdot \text{v}^{-1} \cdot \text{s}^{-1}$ (RSD, 6.4 %) and $7.1 \cdot 10^{-10} \text{ m}^2 \cdot \text{v}^{-1} \cdot \text{s}^{-1}$ (RSD, 3.7 %), and more than one order lower than the EOF mobility of a bare fused silica capillary using 50 mM acetic acid pH 5.0 ($1.9 \cdot 10^{-8} \text{ m}^2 \cdot \text{v}^{-1} \cdot \text{s}^{-1}$ (RSD, 2.4 %). The separation performance and repeatability of the HPMC-coated capillaries were also tested (Section S- III of the Supporting Information).

3.2. CZE method development and evaluation

To achieve efficient charge variant separation of intact mAbs by CZE, the pH of BGE (2.8, 4.0, 5.0, 5.8) and concentration of BGE (10–100 mM acetic acid) were optimized. Acetic acid was used as a BGE constituent due to its volatility and compatibility with MS detection. First, the effect of the pH of the BGE on the CZE analysis of four different mAbs was evaluated. The acetic acid concentration was established at 50 mM in all cases while consistently applying +25 kV as separation voltage. The results obtained for pembrolizumab are depicted in Fig. 1. Electropherograms for the other three mAbs are reported in Fig. S5, and a summary of the results can be found in Table S2. All measurements were performed in triplicates. As shown in Fig. 1A and S5, the pH of the BGE strongly affects the separation of the charge variants. At pH 2.8, no variants are resolved from the main isoform of pembrolizumab, whereas, at pH 5.0 and 5.8, five or six charge variants were observed next to the main isoform peak. The mAb and its charge variants migrate slower as the pH of the BGE approaches the pI of the mAb, due to their reduced net charge and thus decreased electrophoretic mobility. Electrophoretic mobility differences between charge variants depend on their relative net charge difference. The electrophoretic mobility difference is relatively small at low pH (e.g., pH 2.8), especially for acidic variants as these are (partially) protonated at low pH. In contrast, increasing the pH values to 5.0 and 5.8 (i.e., closer to the mAb pI) reduces the net charge of the antibody and increases the relative electrophoretic mobility differences between charge variants, resolving basic and acidic variants from the main isoform (Fig. 1A). The basic variants

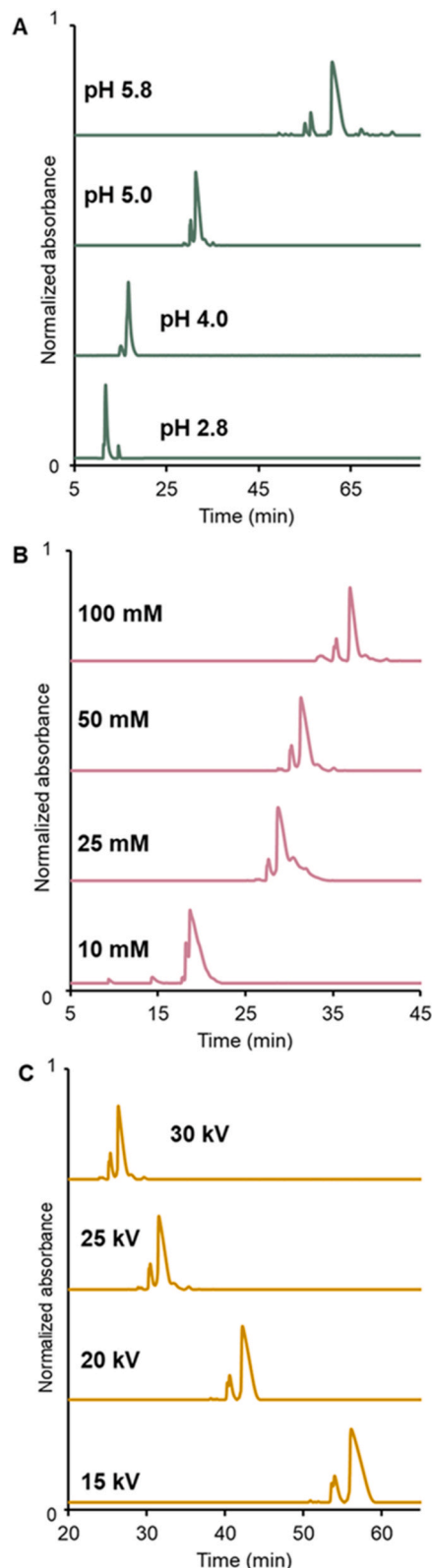


Fig. 1. CZE-UV analysis of pembrolizumab ($1.0 \text{ mg} \cdot \text{mL}^{-1}$) using (A) BGEs of 50 mM acetic acid adjusted to various pH values (2.8–5.8), (B) BGE at various acetic acid concentrations (10–100 mM) adjusted to pH 5.0, and (C) a BGE of 50 mM acetic acid adjusted to pH 5.0 applying various voltages (+15–30 kV). Conditions: HPMC-coated capillary ($50 \mu\text{m}$ i.d. \times 60 cm), BGE 50 mM acetic acid (pH 5.0) (unless stated otherwise), separation voltage +25 kV (A and B). See paragraph 2.4.1 for additional CE conditions and Fig. S5 for the CZE-UV analysis of rituximab, NISTmAb, and cetuximab.

are migrating first as they are more positively charged (higher pI) than the main isoform [5,39]. The acidic variants migrate slower due to their decrease in pI with respect to the main mAb. For example, deamidation introduces negative charges to the antibody and gives it a net lower positive charge [40]. For optimal resolution, the relative difference in electrophoretic mobilities between the charge variants should be maximized. Most resolved charge variants for the mAbs were achieved at pH 5.8. Nevertheless, for the final method conditions, a BGE of pH 5.0 was chosen as a compromise due to a distinctly faster run time (e.g., pembrolizumab migration time of about 31 vs. 61 min at pH 5.0 vs. 5.8, respectively) and lower CZE current obtained (30–35 μA vs. >60 μA at pH 5.0 and 5.8, respectively), which was a preferable choice considering the requirements for CZE-MS.

Next, different BGE concentrations (10–100 mM acetic acid adjusted to pH 5.0) were tested (Fig. 1B and S5). A noticeable increase in migration time with increasing BGE concentrations was observed. The lowest BGE concentration (10 mM) diminished electrophoretic resolution among the charge variants. Conversely, higher BGE concentration resulted in lower effective mobility, maximizing the difference in electrophoretic mobility and allowing for better separation efficiency. Considerably, more charge variants were resolved at higher BGE concentrations (50–100 mM). For example, using 10 mM acetic acid adjusted to pH 5.0 as BGE, no acidic variants were resolved from the main isoform, whereas with 100 mM acetic acid (pH 5.0), three acidic variants were separated (Fig. 1B). Cetuximab has several different sialylated glycoforms which emerge as acidic variants. At 100 mM acetic acid (pH 5.0), six acidic variants could be separated, whereas at a lower BGE concentration (10 mM) only two acidic variants were separated (Fig. S6). This trend of more resolved charge variants at higher BGE concentrations was observed for all tested mAbs. The best separation and highest plate numbers were achieved at 50 and 100 mM acetic acid (pH 5.0) (Fig. S7). The plate numbers were calculated based on the main isoform by using Eq. S1. 50 mM acetic acid (pH 5.0) was selected as the most practical BGE concentration due to hyphenating with MS later on. It should be noted that under the described conditions, the peaks of the mAbs have a triangular peak shape making it challenging to resolve the acidic variants from the main isoform peak (Fig. 1 and S5). The observed triangular peaks arise from the local electric field strength that is higher in the analyte zone compared to the BGE zone [41]. This phenomenon, known as electromigration dispersion, can lead to reduced plate numbers and increased overlap between acidic variants and the main isoform.

To speed up CVA and evaluate the impact of the electric field, various applied voltages (+15–30 kV were tested using 50 mM acetic acid (pH 5.0) as BGE. Evidently, at higher electric fields, faster ion migration (Fig. 1C), and higher currents were observed (e.g., 30 vs. 15 μA at +30 and 15 kV, respectively). Short separation times enhanced separation efficiency (plate numbers) as diminished diffusion correlates with reduced peak broadening. For instance, at 15 kV, the plate number is ~ 1.4 times lower compared to +25 kV (Fig. S7). At the different applied voltages, the number of resolved charge variants peaks was similar (Fig. S6). A voltage of +25 kV was selected as optimal as the plate number was the highest.

In pharmaceutical analysis, maintaining separation performance is paramount, even when dealing with elevated quantities of injected mAb. In the CZE-UV experiments described above, an injected mAb concentration of 1 $\text{mg}\cdot\text{mL}^{-1}$, was used, corresponding to 6.4 ng of total mAb (0.54 % of total capillary length). Fig. 2 shows the CZE separation performance of pembrolizumab as a function of injected concentrations (0.1–5 $\text{mg}\cdot\text{mL}^{-1}$). The charge variant resolution decreases at higher injected concentrations of mAb, resulting in a lower number of resolved peaks (Figs. S8 and S9). At a higher injected concentration (e.g., 5 $\text{mg}\cdot\text{mL}^{-1}$), the acidic variants, in particular, overlap more with the main isoform due to the broader FWHM of the main isoform at higher concentrations (0.55 min vs. 1.29 min for 0.1 and 5 $\text{mg}\cdot\text{mL}^{-1}$ pembrolizumab, respectively) (Table S3). In contrast, the basic variants

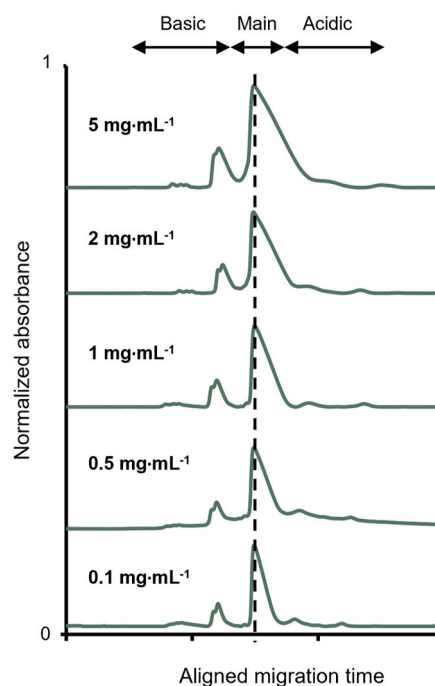


Fig. 2. CZE-UV analysis of pembrolizumab at different injected concentrations (0.1 $\text{mg}\cdot\text{mL}^{-1}$, 0.5 $\text{mg}\cdot\text{mL}^{-1}$, 1 $\text{mg}\cdot\text{mL}^{-1}$, 2 $\text{mg}\cdot\text{mL}^{-1}$, and 5 $\text{mg}\cdot\text{mL}^{-1}$). The migration times of the peaks are aligned based on the top of the peak of the main isoform (black dot line). Conditions: HPMC-coated capillary (50 μm i.d. \times 60 cm), BGE 50 mM acetic acid (pH 5.0), separation voltage +25 kV. See section 2.4.1 for additional CE conditions and Fig. S8 for the CZE-UV analyses of rituximab, NISTmAb, and cetuximab.

remain separated from the main isoform. A lower injected concentration improves the peak shape as the sample is more diluted resulting in less electromigration dispersion. In conclusion, the separation performance can be maintained when an injected concentration of 0.1–2 $\text{mg}\cdot\text{mL}^{-1}$ is used.

3.3. Comparison with established EACA-based CZE-UV method

To benchmark the developed MS-compatible method, the four mAbs described in this study were also measured by applying the EACA method described by He et al. [18]. The EACA method provides a better separation of the basic and acidic variants from the main isoform compared to the MS-compatible method (Figs. 3A and S10). For example, Fig. 3A shows that the basic variants of pembrolizumab are resolved better with the EACA method compared to our MS-compatible method. The relative abundances of the main isoform and basic and acidic variants of four different mAbs were determined with the EACA method and the MS-compatible method (Fig. 3B). There is a clear correlation between the values obtained with both methods (slope of 0.926), indicating that the methods' capacity to distinguish charge variants from the main isoform is similar. For both methods, the injected sample concentration was 1 $\text{mg}\cdot\text{mL}^{-1}$. At this concentration of NIST-mAb, the relative abundance of the basic variants was lower than that obtained with the EACA method. However, when lowering the injected concentration to 0.5 $\text{mg}\cdot\text{mL}^{-1}$, the two methods produced similar relative abundances for the charge variants. As shown in the previous section, this may be attributed to capillary overloading, which may decrease the resolution between the charge variants and the main isoform. Nevertheless, the relative abundances obtained with the two methods were typically quite similar. The largest difference in relative abundance was observed for rituximab (Table S4), which exhibited a relative abundance of the main isoform of 79.3 % and 70.3 % using the EACA and the new method, respectively. On the other hand, the relative

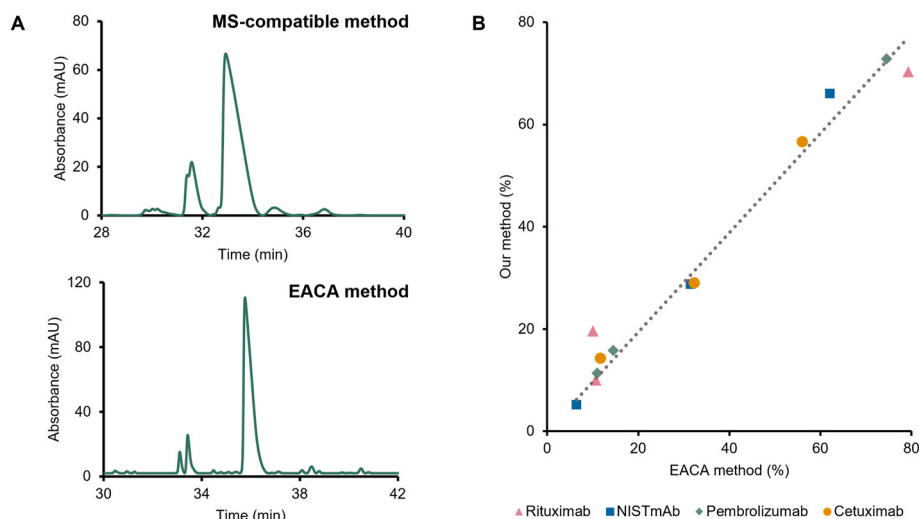


Fig. 3. (A) CZE-UV of $1 \text{ mg}\cdot\text{mL}^{-1}$ pembrolizumab using the MS-compatible method (top, section 2.4.1 for conditions) and the EACA method (bottom, see section 2.4.3. for conditions). (B) Relative peak area percentage (%) of the charge variants of $1 \text{ mg}\cdot\text{mL}^{-1}$ rituximab (pink, triangle), $0.5 \text{ mg}\cdot\text{mL}^{-1}$ NISTmAb (blue, square), $1 \text{ mg}\cdot\text{mL}^{-1}$ pembrolizumab (green, diamond), and $1 \text{ mg}\cdot\text{mL}^{-1}$ cetuximab (yellow, circle) analyzed with the MS-compatible method (y-axis) and the EACA method from He et al. (2011) (x-axis). A trendline (forced intercept = 0) is plotted (grey dots) to express the degree of similarity in relative abundance. The relative abundance values are listed in Table S4. The electropherograms of both methods of rituximab, NISTmAb, and cetuximab are represented in Fig. S10. (For interpretation of the references to colour in this figure legend, the reader is referred to the Web version of this article.)

abundances of the basic variants of pembrolizumab (14.5 % (EACA method) and 15.8 % (our method)) were very similar for both methods.

For the other antibodies, the difference in the relative abundance of the charge variants determined with both methods was never more than 5.9 %. In conclusion, although the relative abundances of charge variants of the four mAbs align closely between different methods and with literature values, minor variations can occur depending on the specific analytical techniques and methodologies used, as highlighted by Goyon et al. (2017) [42].

3.4. Optimization of the CZE-MS method

The nanoCEasy interface was implemented to couple the CZE to MS [33]. In this study, a Q Exactive Plus MS instrument was employed. In our initial experiments, we used direct-infusion measurements of pembrolizumab in to obtain suitable MS parameters for our analysis (see Table S5 for additional experimental information). In particular, the choice of suitable iCID and the S-lens RF levels were critical. We selected S-lens RF level of 100 and iCID, of 80 eV, which provided the best results in terms of signal-to-noise (data not shown).

On Orbitrap instruments, the grounding takes place on the MS orifice; this needs to be considered when developing CE-MS methods, as voltages applied during CE and ESI may interfere. Therefore, to protect the MS instrument and ensure spray stability, BGE systems creating currents above $35 \mu\text{A}$ were avoided. In our experiments, the pH of the BGE was adjusted using ammonium hydroxide ($\sim 5.9 \text{ mM}$ to adjust the pH to 5.0), increasing the ionic strength of the BGE, and therefore, the CE current. Considering the coupling with MS, the use of a BGE buffer containing 50 mM acetic acid (pH 5.8) or 100 mM acetic acid (pH 5.0) could lead to an elevated CE current ($>60 \mu\text{A}$). Because of safety precautions, 50 mM acetic acid (pH 5.0) was chosen as an optimal BGE composition for the separation of charge variants with CZE-MS. An additional challenge with a high CE current was that the actual MS voltage ($>2.1 \text{ kV}$) exceeded the applied MS voltage (2.1 kV), resulting in an unstable ionization. The additional voltage is likely to come from the CE instrument. To address this problem, the CE voltage was reduced to $+20 \text{ kV}$ in order to gain control of the actual MS voltage and to ensure a stable ionization spray.

The syringe pump for the sheath liquid was set to $10 \mu\text{L}\cdot\text{min}^{-1}$, however, only about $100 \text{ nL}\cdot\text{min}^{-1}$ of sheath liquid will enter the emitter

tip [33]. The remaining flow is flushed backward towards the waste as shown in Figs. S1 and S2. Initially, we tested different organic solvents (methanol, acetonitrile, and isopropanol) and types of acid (acetic acid and formic acid) in the sheath liquid. The results were evaluated by assessing the MS signal intensity, charge state distribution, and presence of adducts of $1 \text{ mg}\cdot\text{mL}^{-1}$ pembrolizumab (Fig. S11). No major difference in charge state distribution was observed between the three organic solvents in the sheath liquid. However, the MS signal intensity dropped a factor of 2.5 with acetonitrile in the sheath liquid. The highest signal intensity was obtained with isopropanol. The type of acid used in the sheath liquid (either 0.5 % (v/v) formic or acetic acid in 50/50 isopropanol/water) was also evaluated (Fig. S12). A shifted charge state distribution was observed with acetic acid in the sheath liquid compared to formic acid. This effect is attributed to the higher pH of 0.5 % (v/v) acetic resulting in less charging compared to 0.5 % (v/v) formic acid (lower pKa). It is known that the CZE separation can be affected by differences between the composition of BGE (pH 5.0) and sheath liquid (pH 2–3) [43]. In CZE-MS, it can be advantageous to use the same counterion in the sheath liquid as in the BGE. The charge variants of pembrolizumab, are better separated with 0.5 % (v/v) acetic acid in the sheath liquid as compared to 0.5 % (v/v) formic acid (Figs. S13A–B and S14A–B). However, the peak width of the charge variants is higher due to lower electrophoretic mobility (longer migration time). Furthermore, the signal intensity is higher with 0.5 % formic acid in sheath liquid (about 20x) thanks to better ionization at lower pH. Due to the higher intensity, lower abundant basic variants were better detected with 0.5 % (v/v) formic acid in the sheath liquid (Fig. S14B) while with 0.5 % (v/v) acetic acid in the sheath liquid, the acidic variants were more likely to be separated (Fig. S13A). For example, zero N-terminal pyroglutamate conversion was identified with 0.5 % (v/v) formic acid in sheath liquid which was not the case with 0.5 % (v/v) acetic acid in sheath liquid (Figs. S13B and S14B). This allows the identification of less abundant proteoforms.

As the detection of low-abundant proteoforms in mAbs is crucial, $1 \text{ mg}\cdot\text{mL}^{-1}$ of tested mAbs was employed to ensure the detection of low abundant charge variants. For cetuximab, the concentration was higher ($2 \text{ mg}\cdot\text{mL}^{-1}$) due to its higher heterogeneity. As shown above, the basic variants could be separated from the main isoform. However, there is a loss in separation performance observed for CZE-MS as compared to CZE-UV (Figs. S15–S18). This can be attributed to the presence of a dead

volume between the end of the separation capillary and the emitter tip. Additionally, the type of acid used in the sheath liquid (acetic acid vs. formic acid) potentially negatively impacted the separation performance. With this method, we were able to detect proteoforms down to 0.6 % relative to the main isoform peak which would correspond to 6 $\mu\text{g}\cdot\text{mL}^{-1}$.

3.5. Profiling of mAbs by CZE-MS

Based on the effective electrophoretic mobility (μ_e) of the four mAbs, there is a separation between the identified basic and acidic charge variants (Fig. 4). The basic variants (presence of C-terminal lysine and cyclization of N-terminal pyroglutamate) have a higher effective electrophoretic mobility compared to the acidic variants (sialylation)

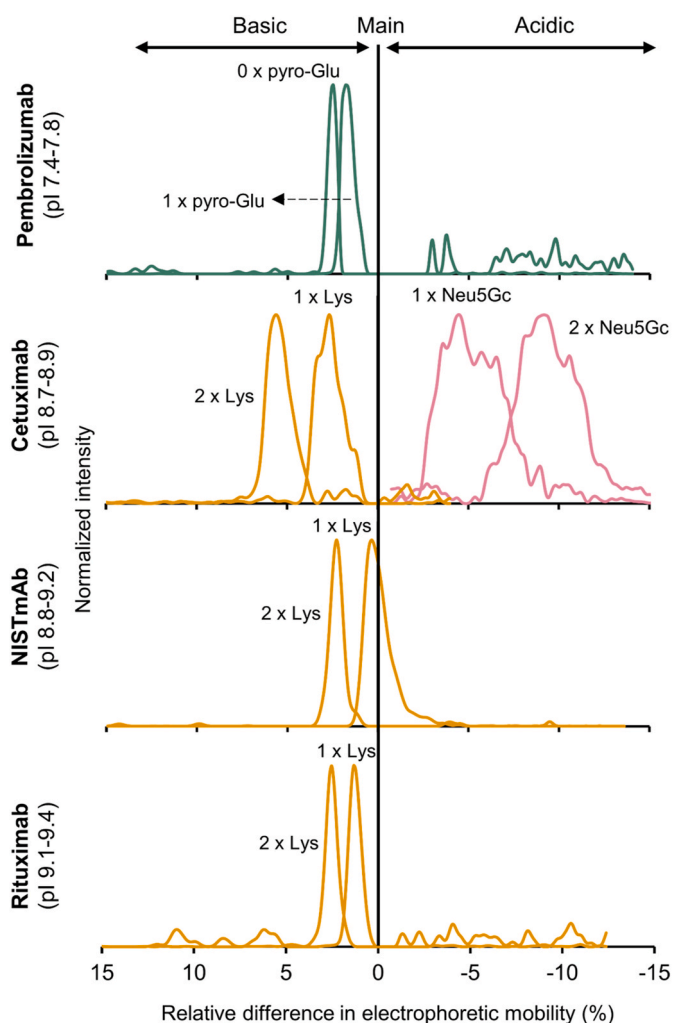


Fig. 4. Separation of basic (cyclization N-terminal pyroglutamate (pyro-Glu) (green), C-terminal lysine residuals (Lys) (yellow)) and acidic variants (sialylated glycoforms (Neu5Gc) (pink)) based on relative difference effective electrophoretic mobility (μ_e) of pembrolizumab, cetuximab, NISTmAb and rituximab (top to bottom). The relative difference in μ_e (%) was calculated with the difference between the μ_e of the charge variants and the main isoform. The μ_e of basic variants is positive (left) to the main isoform and the μ_e of acidic variants is negative (right) to the main isoform. The m/z values of the created EIEs are listed in Table S6. Conditions: HPMC-coated capillary (50 μm i.d. x 60 cm), BGE 50 mM acetic acid (pH 5.0), separation voltage +20 kV, sheath liquid 0.5 % (v/v) formic acid in 50/50 isopropanol/water. See sections 2.4.1 and 2.4.2 for detailed CE and MS settings. (For interpretation of the references to colour in this figure legend, the reader is referred to the Web version of this article.)

(Fig. 4). The EIEs of four mAbs based on specific m/z values and the theoretical and measured masses of the charge variants are listed in Tables S6 and S7, respectively.

C-terminal lysine clipping is a common occurrence during the production process of therapeutic mAb. This process is driven by an enzymatic reaction with carboxypeptidase. However, this reaction is often incomplete, leaving residual lysines on the mAb [44]. A residual C-terminal lysine is indicated by a positive mass offset of 128 Da. The NISTmAb, rituximab, and cetuximab contain residual C-terminal lysine (Lys) from incomplete clipping [31,45,46]. For NISTmAb, there are two basic variants. The second basic variant peak (1 x Lys) partially overlaps with the main isoform peak but can be distinguished through MS data (Fig. S15). The basic variant peaks showed a positive mass offset of one or two times 128 Da (first basic peak (148,461.5 Da, G0F/G1F + 2 Lys)) and (second basic peak (148,330.0 Da, G0F/G1F + 1 Lys)) in comparison to the main isoform peak, indicating to C-terminal lysine variants (Figs. 4 and S15, Table S7). The glycoforms were assigned using the nomenclature reported by Lippold et al. (2019) [47]. The main isoform represents a fully process antibody, where C-terminal lysines have been completely removed. Incomplete C-terminal lysine clipping was also observed for rituximab and cetuximab (Figs. 4, S16, and S17). The basic variants were resolved from the main isoform. For rituximab, oxidation (Ox) was also encountered for the basic variants, resulting in 16 Da mass offset ((peak 2 x Lys (147,510.2 Da, G0F/G1F + 2 Lys + Ox), (main isoform, (147,240.8 Da, G0F/G1F)) (Fig. S16, Table S7). Fig. 4 depicts the separation of the residual C-terminal lysines. The difference in effective electrophoretic mobility of a single C-terminal lysine variant and the main isoform (full clipping) is about $1.0 \cdot 10^{-10} \text{ m}^2 \cdot \text{V}^{-1} \cdot \text{s}^{-1}$. Variants with two residual C-terminal lysine (2 Lys) show a roughly two times higher difference in effective electrophoretic mobility, fitting well with expectations besides NISTmAb.

The majority of the antibodies contain either zero or two conversions of glutamine to pyroglutamate on the heavy chain of the main isoform. This process occurs at the N-terminal end of the heavy chain of amino acid glutamine (Q). However, rituximab contains four times the cyclization of N-terminal pyroglutamate (two times on the heavy chain and twice on the light chain) [48]. Rituximab only showed complete conversion to N-terminal pyroglutamate, whereas pembrolizumab did exhibit partial conversion to N-terminal pyroglutamate. Conversion to N-terminal pyroglutamate loses a positively charged N-terminal amine. This can occur via a chemical or enzymatic reaction. Incomplete conversion to N-terminal pyroglutamate still has this positively charged N-terminal amine, resulting in an increase in pI of the mAb, and is, therefore, a basic charge variant [49]. The basic variants are distinguished from the main isoform, which has a higher effective electrophoretic mobility, contrary to the main isoform ($1.0 \cdot 10^{-8} \text{ m}^2 \cdot \text{V}^{-1} \cdot \text{s}^{-1}$) (Figs. 4 and S18). The first basic variant peak (148928.8 Da, G0F/G0F + 0 x pyro-Glu) contains no conversion to N-terminal pyroglutamate (Table S7). The second basic variant (148907.0 Da, G0F/G0F + 1 x pyro-Glu) exhibits a +17 Da mass shift relative to the main isoform, indicating one-time cyclization to N-terminal pyroglutamate. The main isoform (148890.3 Da, G0F/G0F + 2 x pyro-Glu) contains two cyclizations of N-terminal pyroglutamate. To the best of our knowledge, this is the first time that pembrolizumab has been analyzed with CZE-MS. The identified modifications are in agreement with a recent study by Zhang et al. (2023) in which pembrolizumab was measured using imaged cIEF [50].

The basic variants could be resolved from the main isoform. However, the acidic variants presented a more challenging case due to the greater degree of overlap with the main isoform. In the CZE-UV electropherogram of pembrolizumab, there are clearly two acidic variant peaks visible (Fig. 3A). Deamidation is a small proteoform with a positive mass shift of 1 Da with respect to the main isoform. To determine deamidation variants, the antibodies were also measured at 35,000 resolution. However, only for pembrolizumab, multiple deamidation variants were determined due to a mass difference of 1 Da. For example,

the main isoform (149,376.9 Da (G1F/G2F)) and acidic variant (149,378.1 Da (G1F/G2F with possible deamidation)) were distinguished. This minor mass difference was also observed in two additional glycoforms. The remaining identified glycoforms had a larger mass difference of 2–3 Da (Table S8). Based on separation, these acidic variants were more resolved from the main isoform with 0.5 % (v/v) acetic acid in a 50/50 isopropanol/water sheath liquid composition. The shift in migration time between the main isoform and acidic variants could also indicate the presence of deamidated proteoforms (Fig. S13A). In addition, there is a small m/z shift for the acidic variants relative to the main isoform which is less pronounced for pembrolizumab measured with 0.5 % (v/v) formic acid in the sheath liquid contrary to 0.5 % (v/v) acetic acid in sheath liquid (Figs. S13C and S14C). Analyzing antibodies at the middle-up or bottom-up level can further elucidate deamidation locations [51]. For NISTmAb, glycation was observed, as indicated by a mass difference of 160 Da between the main isoform (148,364.0, G1F/G1F or G0F/G2F) and the acidic variant (148,524.8 Da, G1F/G1F or G0F/G2F), consistent with the addition of a hexose monosaccharide (162 Da). Glycation occurs on the primary amine group of a lysine residue, neutralizing the positive charge. Cetuximab is a more heterogeneous mAb due to a total of four glycosylation sites present in the Fc and Fab domains (each of two glycosylation sites) [52]. Due to the high number of glycoform combinations and isomers, it is more challenging to identify the proteoforms. Our method enables the differentiation of acidic variants from the main isoform of cetuximab ($\mu_e = -3.54$ to $-8.97 \cdot 10^{-10} \text{ m}^2 \cdot \text{V}^{-1} \cdot \text{s}^{-1}$). The acidic variants include sialylated (N-glycolylneuraminic acid (Neu5Gc)) glycoforms (Fig. S17). The Fab region contains murine-type glycans, e.g., Neu5Gc, and was one or two times present on the glycoforms (Table S7). It should be noted that the sialylated glycoforms peaks are broader compared to e.g., residual C-terminal lysine peaks, likely due to the presence of isoforms derived from sialylated glycoforms.

4. Conclusion

From a CQA perspective, it is crucial to monitor charge variants of mAbs. With the CZE-based EACA method pioneered by He et al. (2011), charge variants can be separated and quantified by optical detection. Nonetheless, the identification of these variants by MS is not possible due to the non-volatile BGE. Our developed method not only facilitates relative quantification via optical detection but also enables hyphenation with MS to identify charge variants. Using a higher pH (e.g., pH 5.0 or 5.8), the charge variants were more effectively separated from the main isoform compared to the typical acidic pH (e.g., pH 2.8) conditions used for CZE-MS of proteins. The method was evaluated with several antibodies in the pI range of 7.4–9.4, variation in IgG subclasses (IgG₁ and IgG₄), and with varying degrees of heterogeneity. Thanks to the selectivity of this method, the developed CZE method is applicable for the separation of a variety of charge variants, including incomplete lysine clipping, incomplete pyroglutamate conversion, and sialylated glycoforms. No sample preparation was required. A correlation exists in terms of the relative abundances of the charge variants acquired through the CZE-UV EACA method of He et al. and our method. However, the acidic variants overlapped more with the main isoform with our CZE-UV method than with the EACA method. As with the EACA method, MS detection is not possible due to the use of non-volatile buffers, our CZE-UV/MS method shows flexibility as it can be used for relative quantification as well as identification of the charge variants due to the use of volatile BGE buffers. This highlights the potential of this CZE-UV/MS method to be a valuable tool for in-depth mAb charge variant characterization.

CRedit authorship contribution statement

Annika A.M. van der Zon: Writing – original draft, Visualization, Methodology, Investigation, Conceptualization. **Alisa Höchsmann:**

Resources. **Tijmen S. Bos:** Data curation. **Christian Neusüß:** Resources. **Govert W. Somsen:** Writing – review & editing, Conceptualization. **Kevin Jooß:** Writing – review & editing, Supervision, Conceptualization. **Rob Haselberg:** Writing – review & editing, Conceptualization. **Andrea F.G. Gargano:** Writing – review & editing, Supervision, Project administration, Funding acquisition, Conceptualization.

Declaration of competing interest

The authors declare that they have no known competing financial interests or personal relationships that could have appeared to influence the work reported in this paper.

Acknowledgments

The authors would like to thank Jesper Ruiter (Vrije Universiteit Amsterdam, CASA) for the preliminary experiments on the HPMC coating and Johannes Schlecht (Agilent Technologies) for his help with the nanoCEasy interface.

Appendix B. Supplementary data

Supplementary data to this article can be found online at <https://doi.org/10.1016/j.aca.2024.343287>.

Data availability

The dataset are archived in the MassIVE repository at <https://doi.org/10.25345/C5377662N>.

References

- [1] P. Sharma, R.V. Joshi, R. Pritchard, K. Xu, M.A. Eicher, Therapeutic antibodies in medicine, *Molecules* 28 (2023) 6438, <https://doi.org/10.3390/molecules28186438>.
- [2] H. Liu, G. Gaza-Bulseco, D. Faldu, C. Chumsae, J. Sun, Heterogeneity of monoclonal antibodies, *J. Pharmacol. Sci. (Tokyo, Jpn.)* 97 (2008) 2426–2447, <https://doi.org/10.1002/jps.21180>.
- [3] T. Gupta, A. Kumar, S. Seshadri, Bioprocess challenges in purification of therapeutic protein charge variants, *Biotechnol. Bioproc. Eng.* 28 (2023) 493–506, <https://doi.org/10.1007/s12257-023-0078-4>.
- [4] A. Beck, H. Liu, Macro- and micro-heterogeneity of natural and recombinant IgG antibodies, *Antibodies* 8 (2019) 18, <https://doi.org/10.3390/antib8010018>.
- [5] Y. Du, A. Walsh, R. Ehrick, W. Xu, K. May, H. Liu, Chromatographic analysis of the acidic and basic species of recombinant monoclonal antibodies, *mAbs* 4 (2012) 578–585, <https://doi.org/10.4161/mabs.21328>.
- [6] A.A.M. van der Zon, J. Verduin, R.S. van den Hurk, A.F.G. Gargano, B.W.J. Pirok, Sample transformation in online separations: how chemical conversion advances analytical technology, *Chem. Commun.* 60 (2024) 36–50, <https://doi.org/10.1039/D3CC03599A>.
- [7] S. Pot, C. Gstöttner, K. Heinrich, S. Hoelzerhoff, I. Grunert, M. Leiss, et al., Fast analysis of antibody-derived therapeutics by automated multidimensional liquid chromatography – mass spectrometry, *Anal. Chim. Acta* 1184 (2021) 339015, <https://doi.org/10.1016/j.aca.2021.339015>.
- [8] S. Fekete, A. Beck, J.-L. Veuthey, D. Guillaume, Ion-exchange chromatography for the characterization of biopharmaceuticals, *J. Pharm. Biomed. Anal.* 113 (2015) 43–55, <https://doi.org/10.1016/j.jpba.2015.02.037>.
- [9] H. Kaur, J. Beckman, Y. Zhang, Z.J. Li, M. Sziget, A. Guttman, Capillary electrophoresis and the biopharmaceutical industry: therapeutic protein analysis and characterization, *TrAC, Trends Anal. Chem.* 144 (2021) 116407, <https://doi.org/10.1016/j.trac.2021.116407>.
- [10] J. Kahle, H. Wätzig, Determination of protein charge variants with (imaged) capillary isoelectric focusing and capillary zone electrophoresis, *Electrophoresis* 39 (2018) 2492–2511, <https://doi.org/10.1002/elps.201800079>.
- [11] T. Xu, L. Sun, A mini review on capillary isoelectric focusing-mass spectrometry for top-down proteomics, *Front. Chem.* 9 (2021), <https://doi.org/10.3389/fchem.2021.651757>.
- [12] M. Dadouch, Y. Ladner, C. Perrin, Analysis of monoclonal antibodies by capillary electrophoresis: sample preparation, separation, and detection, *Separations* 8 (2021) 4, <https://doi.org/10.3390/separations8010004>.
- [13] K. Jooß, J.P. McGee, R.D. Melani, N.L. Kelleher, Standard procedures for native CZE-MS of proteins and protein complexes up to 800 kDa, *Electrophoresis* 42 (2021) 1050–1059, <https://doi.org/10.1002/elps.202000317>.
- [14] R. Haselberg, T. De Vijlder, R. Heukers, M.J. Smit, E.P. Romijn, G.W. Somsen, et al., Heterogeneity assessment of antibody-derived therapeutics at the intact and middle-up level by low-flow sheathless capillary electrophoresis-mass

- spectrometry, *Anal. Chim. Acta* 1044 (2018) 181–190, <https://doi.org/10.1016/j.aca.2018.08.024>.
- [15] J. Kiraga, P. Mackiewicz, D. Mackiewicz, M. Kowalczyk, P. Biecek, N. Polak, et al., The relationships between the isoelectric point and: length of proteins, taxonomy and ecology of organisms, *BMC Genom.* 8 (2007) 163, <https://doi.org/10.1186/1471-2164-8-163>.
- [16] M.K. Menon, A.L. Zydny, Measurement of protein charge and ion binding using capillary electrophoresis, *Anal. Chem.* 70 (1998) 1581–1584, <https://doi.org/10.1021/ac970902r>.
- [17] S. Meyer, D. Clases, R. Gonzalez de Vega, M.P. Padula, P.A. Doble, Separation of intact proteins by capillary electrophoresis, *Analyst* 147 (2022) 2988–2996, <https://doi.org/10.1039/D2AN00474G>.
- [18] Y. He, C. Isele, W. Hou, M. Ruesch, Rapid analysis of charge variants of monoclonal antibodies with capillary zone electrophoresis in dynamically coated fused-silica capillary, *J. Separ. Sci.* 34 (2011) 548–555, <https://doi.org/10.1002/jssc.201000719>.
- [19] R. Wiesner, H. Zagst, W. Lan, S. Bigelow, P. Holper, G. Hübner, et al., An interlaboratory capillary zone electrophoresis-UV study of various monoclonal antibodies, instruments, and ϵ -aminocaproic acid lots, *Electrophoresis* 44 (2023) 1247–1257, <https://doi.org/10.1002/elps.202200284>.
- [20] H.A. Alhazmi, M. Albratty, Analytical techniques for the characterization and quantification of monoclonal antibodies, *Pharmaceuticals* 16 (2023) 291, <https://doi.org/10.3390/ph16020291>.
- [21] J. Dai, J. Lamp, Q. Xia, Y. Zhang, Capillary isoelectric focusing-mass spectrometry method for the separation and online characterization of intact monoclonal antibody charge variants, *Anal. Chem.* 90 (2018) 2246–2254, <https://doi.org/10.1021/acs.analchem.7b04608>.
- [22] J. Hühner, M. Lämmerhofer, C. Neusüß, Capillary isoelectric focusing-mass spectrometry: coupling strategies and applications, *Electrophoresis* 36 (2015) 2670–2686, <https://doi.org/10.1002/elps.201500185>.
- [23] C. Nagy, M. Andrási, N. Hamidli, G. Gyémánt, A. Gáspár, Top-down proteomic analysis of monoclonal antibodies by capillary zone electrophoresis-mass spectrometry, *Journal of Chromatography Open* 2 (2022) 100024, <https://doi.org/10.1016/j.jcoa.2021.100024>.
- [24] A. Schwenzer, L. Kruse, K. Jooß, C. Neusüß, Capillary electrophoresis-mass spectrometry for protein analyses under native conditions: current progress and perspectives, *Proteomics* 24 (2024), <https://doi.org/10.1002/pmic.202300135>.
- [25] V. Le-Minh, N.T. Tran, A. Makky, V. Rosilio, M. Taverna, C. Smadja, Capillary zone electrophoresis-native mass spectrometry for the quality control of intact therapeutic monoclonal antibodies, *J. Chromatogr. A* 1601 (2019) 375–384, <https://doi.org/10.1016/j.chroma.2019.05.050>.
- [26] X. Shen, Z. Liang, T. Xu, Z. Yang, Q. Wang, D. Chen, et al., Investigating native capillary zone electrophoresis-mass spectrometry on a high-end quadrupole-time-of-flight mass spectrometer for the characterization of monoclonal antibodies, *Int. J. Mass Spectrom.* 462 (2021) 116541, <https://doi.org/10.1016/j.ijms.2021.116541>.
- [27] C. Gstöttner, A. Knaupp, G. Vidarsson, D. Reusch, T. Schlothauer, M. Wührer, et al., Affinity capillary electrophoresis – mass spectrometry permits direct binding assessment of IgG and Fc γ RIIIa in a glycoform-resolved manner, *Front. Immunol.* 13 (2022), <https://doi.org/10.3389/fimmu.2022.980291>.
- [28] S. Carrillo, C. Jakes, J. Bones, In-depth analysis of monoclonal antibodies using microfluidic capillary electrophoresis and native mass spectrometry, *J. Pharm. Biomed. Anal.* 185 (2020) 113218, <https://doi.org/10.1016/j.jpba.2020.113218>.
- [29] Q. Sun, L. Wang, N. Li, L. Shi, Characterization and monitoring of charge variants of a recombinant monoclonal antibody using microfluidic capillary electrophoresis-mass spectrometry, *Anal. Biochem.* 625 (2021) 114214, <https://doi.org/10.1016/j.ab.2021.114214>.
- [30] Z. Wu, H. Wang, J. Wu, Y. Huang, X. Zhao, J.B. Nguyen, et al., High-sensitivity and high-resolution therapeutic antibody charge variant and impurity characterization by microfluidic native capillary electrophoresis-mass spectrometry, *J. Pharm. Biomed. Anal.* 223 (2023) 115147, <https://doi.org/10.1016/j.jpba.2022.115147>.
- [31] F. Füssl, A. Trappe, S. Carrillo, C. Jakes, J. Bones, Comparative elucidation of cetuximab heterogeneity on the intact protein level by cation exchange chromatography and capillary electrophoresis coupled to mass spectrometry, *Anal. Chem.* 92 (2020) 5431–5438, <https://doi.org/10.1021/acs.analchem.0c00185>.
- [32] A.M. MacDonald, C.A. Lucy, Highly efficient protein separations in capillary electrophoresis using a supported bilayer/diblock copolymer coating, *J. Chromatogr. A* 1130 (2006) 265–271, <https://doi.org/10.1016/j.chroma.2006.05.042>.
- [33] J. Schlecht, A. Stolz, A. Hofmann, L. Gerstung, C. Neusüß, nanoCEasy: an easy, flexible, and robust nanoflow sheath liquid capillary electrophoresis-mass spectrometry interface based on 3D printed parts, *Anal. Chem.* 93 (2021) 14593–14598, <https://doi.org/10.1021/acs.analchem.1c03213>.
- [34] Y. Shen, R.D. Smith, High-resolution capillary isoelectric focusing of proteins using highly hydrophilic-substituted cellulose-coated capillaries, *J. Microcolumn Sep.* 12 (2000) 135–141, [https://doi.org/10.1002/\(SICI\)1520-667X\(2000\)12:3<135::AID-MCS2>3.0.CO;2-141](https://doi.org/10.1002/(SICI)1520-667X(2000)12:3<135::AID-MCS2>3.0.CO;2-141).
- [35] S.-J. Baek, A. Park, Y.-J. Ahn, J. Choo, Baseline correction using asymmetrically reweighted penalized least squares smoothing, *Analyst* 140 (2015) 250–257, <https://doi.org/10.1039/C4AN01061B>.
- [36] L.E. Niezen, P.J. Schoenmakers, B.W.J. Pirok, Critical comparison of background correction algorithms used in chromatography, *Anal. Chim. Acta* 1201 (2022) 339605, <https://doi.org/10.1016/j.aca.2022.339605>.
- [37] M.T. Marty, A.J. Baldwin, E.G. Marklund, G.K.A. Hochberg, J.L.P. Benesch, C. V. Robinson, Bayesian deconvolution of mass and ion mobility spectra: from binary interactions to polydisperse ensembles, *Anal. Chem.* 87 (2015) 4370–4376, <https://doi.org/10.1021/acs.analchem.5b00140>.
- [38] L. Hajba, A. Guttman, Recent advances in column coatings for capillary electrophoresis of proteins, *TrAC, Trends Anal. Chem.* 90 (2017) 38–44, <https://doi.org/10.1016/j.trac.2017.02.013>.
- [39] L. Alekseychik, C. Su, G.W. Becker, M.J. Treuheit, V.I. Razinkov, High-throughput screening and analysis of charge variants of monoclonal antibodies in multiple formulations, *SLAS Discovery* 22 (2017) 1044–1052, <https://doi.org/10.1177/2472555217711666>.
- [40] B. Moritz, V. Locatelli, M. Niess, A. Bathke, S. Kiessig, B. Entler, et al., Optimization of capillary zone electrophoresis for charge heterogeneity testing of biopharmaceuticals using enhanced method development principles, *Electrophoresis* 38 (2017) 3136–3146, <https://doi.org/10.1002/elps.201700145>.
- [41] J. Gysler, U. Jaehde, W. Schunack, Electromigration peak dispersion of isotachophoretic protein zones during capillary zone electrophoresis, *Fresenius' J. Anal. Chem.* 365 (1999) 398–403, <https://doi.org/10.1007/s002160051630>.
- [42] A. Goyon, M. Excoffier, M.-C. Janin-Bussat, B. Bobaly, S. Fekete, D. Guillaume, et al., Determination of isoelectric points and relative charge variants of 23 therapeutic monoclonal antibodies, *J. Chromatogr. B* 1065–1066 (2017) 119–128, <https://doi.org/10.1016/j.jchromb.2017.09.033>.
- [43] Frantisek Foret, T.J. Thompson, Vouros Paul, B.L. Karger, Gebauer Petr, Bocek Petr, Liquid sheath effects on the separation of proteins in capillary electrophoresis/electrospray mass spectrometry, *Anal. Chem.* 66 (1994) 4450–4458, <https://doi.org/10.1021/ac00096a010>.
- [44] T.S. Raju, C-Terminal Lys or arg clipping in proteins, in: Co- and Post-Translational Modifications of Therapeutic Antibodies and Proteins, Wiley, 2019, pp. 31–33, <https://doi.org/10.1002/9781119053354.ch3>.
- [45] C.-H. Chen, H. Feng, R. Guo, P. Li, A.K.C. Laserna, Y. Ji, et al., Intact NIST monoclonal antibody characterization—proteoforms, glycoforms—using CE-MS and CE-LIF, *Cogent Chem* 4 (2018) 1480455, <https://doi.org/10.1080/23312009.2018.1480455>.
- [46] F. Di Marco, T. Berger, W. Esser-Skala, E. Rapp, C. Regl, C.G. Huber, Simultaneous monitoring of monoclonal antibody variants by strong cation-exchange chromatography hyphenated to mass spectrometry to assess quality attributes of rituximab-based biotherapeutics, *Int. J. Mol. Sci.* 22 (2021) 9072, <https://doi.org/10.3390/ijms22169072>.
- [47] S. Lippold, S. Nicolardi, M. Wührer, D. Falck, Proteoform-resolved Fc γ RIIIa binding assay for Fab glycosylated monoclonal antibodies achieved by affinity chromatography mass spectrometry of Fc moieties, *Front. Chem.* 7 (2019), <https://doi.org/10.3389/fchem.2019.00698>.
- [48] A. Hinterholzer, V. Stanojlovic, C. Cabrele, M. Schubert, Unambiguous identification of pyroglutamate in full-length biopharmaceutical monoclonal antibodies by NMR spectroscopy, *Anal. Chem.* 91 (2019) 14299–14305, <https://doi.org/10.1021/acs.analchem.9b02513>.
- [49] Z. Liu, J. Valente, S. Lin, N. Chennamsetty, D. Qiu, M. Bolgar, Cyclization of N-terminal glutamic acid to pyro-glutamic acid impacts monoclonal antibody charge heterogeneity despite its appearance as a neutral transformation, *J. Pharmacol. Sci. (Tokyo, Jpn.)* 108 (2019) 3194–3200, <https://doi.org/10.1016/j.xphs.2019.05.023>.
- [50] X. Zhang, T. Kwok, M. Zhou, M. Du, Y. Li, T. Bo, et al., Imaged capillary isoelectric focusing (icIEF) tandem high resolution mass spectrometry for charged heterogeneity of protein drugs in biopharmaceutical discovery, *J. Pharm. Biomed. Anal.* 224 (2023) 115178, <https://doi.org/10.1016/j.jpba.2022.115178>.
- [51] B. Spanov, N. Govorukhina, N. van de Merbel, R. Bischoff, Analytical tools for the characterization of deamidation in monoclonal antibodies, *Journal of Chromatography Open* 2 (2022) 100025, <https://doi.org/10.1016/j.jcoa.2021.100025>.
- [52] M. Biacchi, R. Gahoual, N. Said, A. Beck, E. Leize-Wagner, Y.-N. François, Glycoform separation and characterization of cetuximab variants by middle-up off-line capillary zone electrophoresis-UV/electrospray ionization-MS, *Anal. Chem.* 87 (2015) 6240–6250, <https://doi.org/10.1021/acs.analchem.5b00928>.